

# V Flow

## Technical White Paper

Du Yigang

Ultrasound Imaging System Development Department, Mindray

# Content

.....	1
Introduction.....	3
CFM application in vascular .....	3
CFM faces challenge.....	3
V Flow changes the way .....	3
Technology.....	3
CFM working principle.....	3
CFM technical limits.....	4
V Flow works differently .....	4
Innovative display technology .....	5
Calculation of Wall Shear Stress (WSS) based on V Flow .....	5
Calculation of Oscillatory Shear Index (OSI) based on the WSS .....	6
Calculation of Blood Flow Turbulence based on Vector Velocities .....	6
Calculation of Vascular Strain.....	6
Clinical values of V Flow .....	6
Clinical case studies of V Flow vs CFM.....	7
Quantitative measures provided by V Flow .....	7
Review of clinical studies based on V Flow .....	8
Conclusion .....	9
Acknowledgement .....	9
Reference .....	9

# V Flow

## High Frame Rate Vector Flow Imaging:

A novel visualization of blood flow and advanced hemodynamic measurements

### Introduction

#### CFM application in vascular

Ultrasound color flow mapping (shortening as CFM) has been extensively used in clinical diagnosis. Velocity of blood flow is calculated through a lag-one auto-correlation [1] method using the beamformed and filtered receiving signals. The magnitude of velocity relative to the direction of ultrasound beam propagation can be obtained and thus is applicable to detecting a laminar flow, which is widespread in the human blood circulatory system. A typical instance can be found in the carotid artery, where the flow pattern is close to a parabolic profile. The maximum velocity can be calculated by an angle correction for the measured value. Similarly, the laminar flow is also found in some fairly large and straight arteries, such as the femoral artery, cerebral artery, brachial artery, and abdominal aortic artery, as well as a number of veins. A maximum blood velocity at peak systole associated with spectral Doppler analysis and a high resolution B-mode image can usually be employed to diagnose arterial plaques [2,3].

#### CFM faces challenge

However, not only the laminar flow, but also a more complicated flow can be discovered in some bifurcations or bended vessels, such as carotid bifurcation and bulb. Some studies [4-6] have shown that formation and growth of arterial plaques is particularly prone to taking place in a vessel with a complicated shape, where a vortex flow can be found. Such complex flows cannot be detected by conventional CFM as it only measures a

one-dimensional velocity. Moreover, the laminar flow will completely change even in a long and straight vessel when the flow is blocked by a plaque. Investigation of blood flow, particularly in pathological or curved vessels, requires an advanced flow-measuring method, where both the absolute magnitude of the velocity and the flow direction should be obtained for an optimal diagnosis.

#### V Flow changes the way

In our new generation device, a novel ultrasound-based technology called V Flow will be demonstrated that can dynamically visualize the blood flow, avoiding the inconvenience of angiography. Rather than a series of static images, the fluidity will be displayed with dynamic arrows indicating the flow process. Both the magnitude and direction of the flow can be measured at any location in the vessel.

### Technology

#### CFM working principle

In CFM, ultrasound beams are emitted into the region of interest (ROI). One color image line requires multiple transmissions since the velocity has to be estimated using as many samples as possible to increase the accuracy. The number of samples used is called the ensemble size and is usually 8 to 16, with a compromise of accuracy and frame rate. One image contains a number of image lines and each color line needs many emissions. Thus, the frame rate of a color Doppler image is decreased by a factor of ensemble

size compared to a normal gray-scale B-mode image.

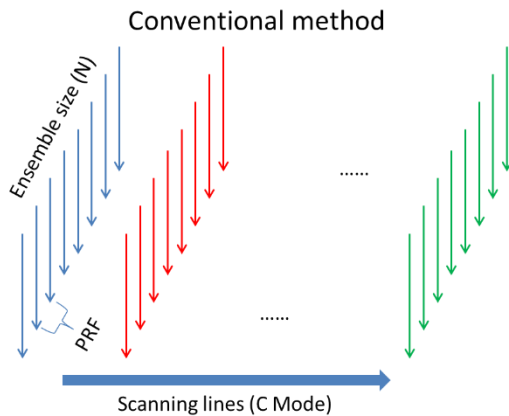


Fig. 1: Scan sequence of conventional CFM

### CFM technical limits

By increasing the pulse repetition frequency (PRF), the frame rate of the color Doppler image can be increased. This also increases the maximum detectable velocity and reduces the aliasing problem. However, the PRF is also restricted to the maximum scanning depth as there has to be enough time for a round trip of the wave. For example, examination of a common carotid artery requires an image display with a depth of 4 to 5 cm. The maximum PRF is then around 15kHz, which is calculated by  $PRF = 1/(Depth \times 2/c)$ , where  $c$  is sound speed with an average of 1540 m/s in human tissue. If the ensemble size is 10, then the frame rate will be around 15 Hz for an image with 100 lines. This process is also illustrated in Fig. 1. The temporal resolution is low for some arteries with high velocities such as the carotid artery, particularly when there is a stenosis. Another drawback is that the time interval for line-by-line scanning is extremely long for the color Doppler imaging due to multiple transmissions of one line. This results in an asynchronous display of a color image since each image line denotes the velocity at a different time. To increase the frame rate and reduce the time difference among image lines, multiple image lines should be beamformed at one transmission. This is the major limitation for a conventional ultrasound platform as it requires a huge amount of data to be

processed in very short time.

### V Flow works differently

In Mindray's ultrasound Resona system, a much more powerful and newly structured platform with an extremely high frequency is used, and is very flexible due to the availability of arbitrary beamforming methods. Therefore, multiple image lines will be generated after a single transmission, and continuous Doppler transmission scanning is applied for the same region of interest, thus continuous clutter filtering can be achieved, to avoid a transient state compared to the conventional color Doppler imaging.

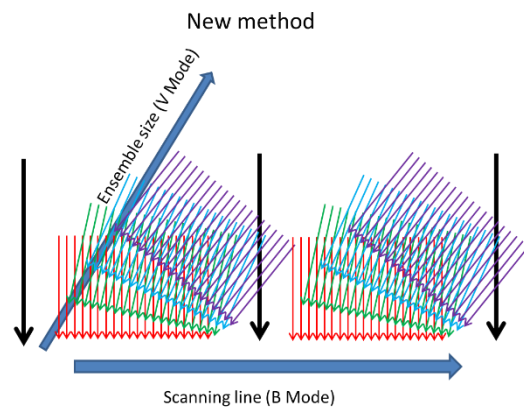


Fig. 2: Scan sequence of V Flow

To derive the direction of velocity of flow at any location, multidirectional transmissions and receptions are employed as shown in Fig. 2, and then a true velocity with accurate direction can be calculated by an angle-compounding technology as shown in Fig. 3, which shows an example where compounding and regression analysis of two angles is applied giving more angles, resulting in an over-determined system [7-9]. The velocities at any location are obtained as long as the area is scanned by the multi-directional beams. Focused beams are also transmitted alternatively and used to generate B-mode image lines. The interleaved transmissions with multidirectional and focused beams, ensure both high-sensitivity vector flow imaging and high-resolution B-mode imaging, respectively [10].

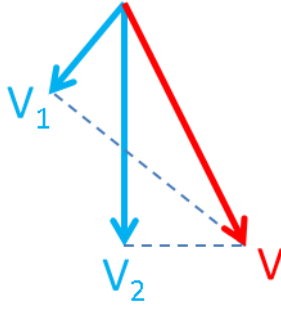


Fig. 3: Example for velocity obtained from two beams. Both the velocity and direction are obtained from an angle compounding technique,

where  $V$  is the compounding velocity, and  $V_1$  and  $V_2$  are Doppler measured velocities.

### Innovative display technology

In order to demonstrate the blood flow more intuitively, an innovative display has been developed [7]. The vector velocities at arbitrary locations within the ROI can be derived at each time instance and thus the fluidity of blood can be achieved by continuously updating the positions of detected red blood cells in the vessel according to the calculated vector velocities as shown in Fig. 4. In this system, colored arrows are used to present both velocity and direction of the flow. The length of the arrow also denotes the velocity. The quantitative values including velocities and their directions can be shown where the cursor is located as presented in Fig. 5 [11]. An adjustable ROI can be manipulated arbitrarily by users, where the maximum and mean velocities are displayed, and the variance of the flow angles inside ROI is calculated, which is a good way to give a quantitative measure for the turbulence. The vector flow results can be displayed slower than real-time with an ultra-high frame rate up to over 400 Hz, so complex flow patterns with an extremely high velocity can be captured [7,8]. Snapshots for flows such as laminar, turbulent, secondary, vortex and contra flows can be demonstrated intuitively in this unique imaging technology, an integral part of the ultrasound diagnostic V Flow system.

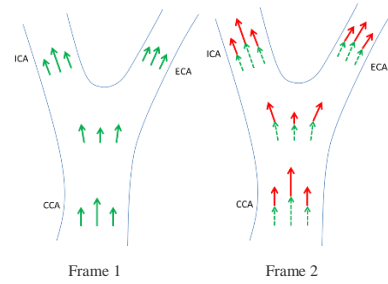


Fig. 4: Dynamic display of vector arrows. Left figure: Frame 1, green arrows indicate current flow velocity and direction and right figure: Frame 2, red arrows represent flow moves forward from the dotted green arrows which correspond to green arrows in Frame 1. CCA: common carotid artery; ICA: internal carotid artery; ECA: external carotid artery.

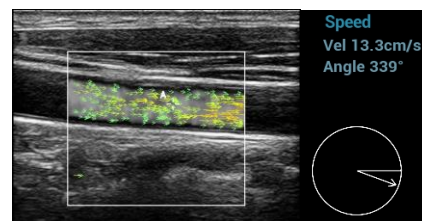


Fig. 5: The velocity and its direction are shown with their physical units at the right image parameter display area. The parameters are updating as a function of frames and places where the cursor is located.

## Calculation of Wall Shear Stress (WSS) based on V Flow

Wall Shear Stress (WSS) is an important parameter for clinical studies of arterial diseases. There are various clinical researches [12-14] using the WSS as an evaluating key factor presenting the relation between the WSS and different arterial diseases. Conventional method for calculating WSS is based on MRI. For V Flow's new generation, the WSS is calculated using ultrasound, which is more convenient and much easier to be obtained. The algorithm can be formulated by [15-17]

$$\tau = \mu \left. \frac{\partial v}{\partial r} \right|_{r=R}$$

Where  $\tau$  is the WSS,  $\mu$  is the blood viscosity,  $v$  is the blood flow velocity calculated by V Flow. The WSS is calculated at a position  $r=R$ , normally on the wall of

the vessel (intima).

## Calculation of Oscillatory Shear Index (OSI) based on the WSS

The oscillatory shear index (OSI) reflects the degree of change in WSS direction over a period of time, e.g., one or several cardiac cycles, and is calculated using the following equation [18,19],

$$OSI = \frac{1}{2} \left( 1 - \frac{\left| \int_0^T \tau dt \right|}{\int_0^T |\tau| dt} \right)$$

Where T represents one cardiac cycle, which can also be a period of time defined. OSI has no physical unit and varies in the range of 0 to 0.5. When there is no change in the direction of WSS within a cardiac cycle, OSI is 0; If there is a change in WSS direction, the OSI is greater than 0 and the maximum value does not exceed 0.5.

## Calculation of Blood Flow Turbulence based on Vector Velocities

The parameter - Turbulen. in V Flow, reflects the degree of blood flow turbulence within a user-defined region of interest (ROI). The calculation equation is as follows [20],

$$Turbulen. = 1 - \frac{\sqrt{C^2 + S^2}}{N}$$

Where  $C = \sum_{i=1}^{i=N} \cos \theta_i$ ,  $S = \sum_{i=1}^{i=N} \sin \theta_i$ . N is the number of points in the ROI,  $\theta_i$  is the angle of the blood flow velocity at the ith point. The parameter - Turbulen. has no physical unit and varies from 0 to 1. The greater the degree of blood flow turbulence, the larger the Turbulen. value. The Turbulen. is 0 or tends to 0 for a pure laminar flow or an approximate laminar flow.

## Calculation of Vascular Strain

Strain is considered the degree of deformation of an object under external forces, and it is the relative deformation of the object in its local area. Vascular strain can reflect the healthy status of the vessel. The strain of long axis blood vessels is related to the length change along the direction of the blood vessel wall, which can be obtained based on the length change of the vessel wall in the longitudinal direction. The calculation equation is as follows [21,22]

$$\varepsilon = \frac{\Delta L}{L_0}$$

Where  $\varepsilon$  is vascular strain,  $\Delta L$  is the length change along the direction of the vascular wall, and  $L_0$  is the initial length.

## Clinical values of V Flow

- Millisecond level temporal resolution which can detect the tiny hemodynamic changes and provide more valuable information than conventional color Doppler
- Grayscale display intuitively shows the spatial distribution of blood flow, which shows better flow sensitivity than conventional power Doppler
- Arrow color/ length, and direction indicate blood flow velocity and direction respectively which helps doctors easily capture abnormal hemodynamics change
- Complex flow imaging illustrating laminar, vortex, secondary, and retrograde flows allows better understanding hemodynamics in different conditions
- Quantitative measurement of velocity and direction at an arbitrary location, and display for velocity curves at three different locations in the same cardiac cycle and same moment, minimizes time-domain influence factors and improves measurement accuracy
- Three measurements of volume flow

implemented based on vector flow imaging offers more precise volume flow value

- Wall Shear Stress (WSS) calculation at three locations based on vector flow imaging opens a new way in studying early plaque development

## Clinical case studies of V Flow vs CFM

V Flow has been applied to different types of flow in the carotid artery to find any difference in comparison to the conventional CFM method.

Case1. Laminar flow occurs in the flat carotid artery as shown in Fig. 6 - Angle steering for CFM

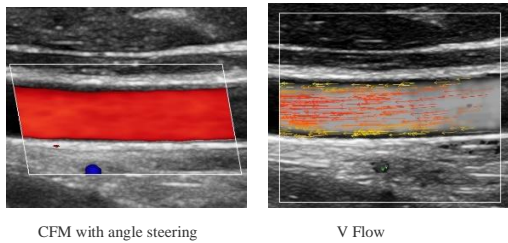


Fig. 6: Laminar flow at CCA. CCA is parallel to the probe surface and steered angle is used in conventional CFM. It shows a uniform forward flow towards the probe. The laminar flow profile cannot be interpreted. In contrast, V Flow not only indicates the flow direction with intuitive arrows, but also represents the character of laminar flow, meaning fast flow in the center and slow flow near the vessel wall.

Case2. Hemodynamics in CCA, ICA, ECA and jugular vein as shown in Fig. 7

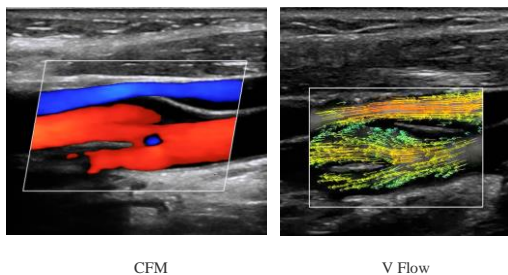


Fig. 7: Jugular vein and carotid bifurcation where the CCA, ICA and ECA are shown in one image. CFM shows flow in Jugular vein and carotid artery run different directions but lacks of detailed hemodynamic. Differently, V Flow not only see flow direction intuitively, but also the flow velocity change in Jugular vein and carotid. Jugular vein as the white arrow points has brighter color than carotid artery. It tells the flow in Jugular vein flow speed faster than in the carotid

artery, which can't be derived from CFM.

## Quantitative measures provided by V Flow

V Flow can provide unique quantitative measurements, including velocities curves (Fig. 8), volume flow (Fig. 9), and WSS (Fig. 10) for clinical studies.

Three velocity curves along with time are plotted at the bottom of the image as shown in Fig. 8.

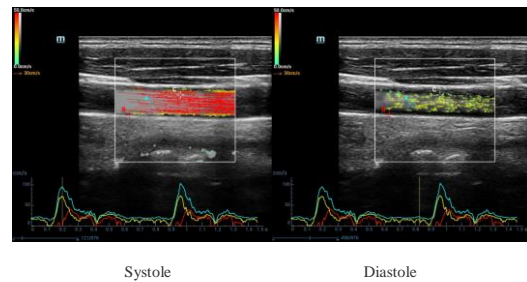


Fig. 8: Three velocity-time curves at three different places are shown. At systole,  $t = 0.2s$  (see the yellow line indicator at the time line), the velocities become maximum and the arrows become long and turn to red. At diastole,  $t = 0.82s$ , the velocities become much smaller and the arrows become short and turn to yellow and green. Note that the velocity magnitude is also displayed with its corresponding color according to the upper left colorbar. The three velocities curves are different since the curve A is at the middle of the vessel and bigger than others which are closed to the vessel wall.

Measurement of volume flow for carotid artery as shown in Fig. 9.

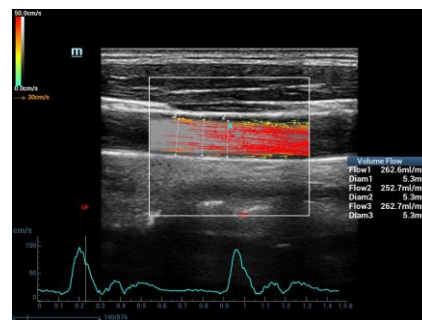


Fig. 9: Three measurements can be made for volume flow at the same image. The cardiac cycle is selected by VF and VF' in terms of the velocity curve as shown at the bottom of the image. Therefore, the volume flow is calculated according to one cardiac cycle based on vector flow velocities. The diameter is also shown along with the volume flow as presented in right middle of the image.

WSS measurements at three different places as shown

in Fig. 10.

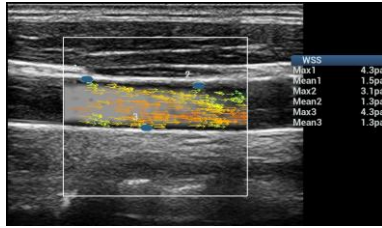


Fig. 10: Three WSS measurements are made at three different places. At each measurement, the maximum and mean values are shown at the right middle of the image.

Multiple results can be obtained and shown simultaneously

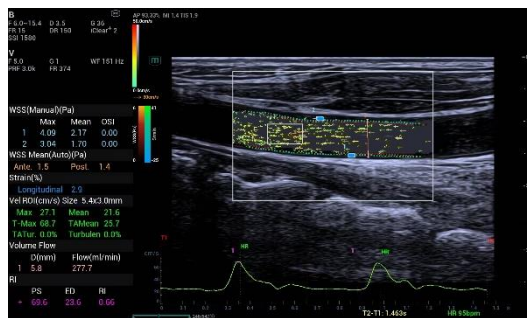


Fig. 10: Based on the saved V Flow video, multiple parameters can be measured quantitatively, including volume flow, resistance index (RI), wall shear stress (WSS), and longitudinal vascular strain.

## Review of clinical studies based on V Flow

The hemodynamic quantitative measurement functions provided by V Flow, including parameters such as WSS, OSI, and Turbulen., have been widely used in clinical researches of peripheral blood vessels (carotid artery, femoral artery, arteriovenous fistula, etc.). As shown in Figs. 12 and 13, WSS at the carotid bulb (CB) due to the presence of low velocity vortex is usually lower than that at the CCA. Similarly, the Turbulen. value at the CB is usually higher than that at the CCA. The hemodynamic differences caused by different vascular shape are worth conducting more in-depth research with a larger sample size. A review of V Flow-based clinical studies will be presented in

the following.

Qiu et al. 2020 [23] measured the WSS of the common carotid artery in 80 healthy volunteers, where the reliability study of the article showed that the intraclass correlation coefficients (ICC) for groups with different ages were all above 0.9. A study of 51 cases of carotid artery stenosis by Qiu et al. in 2021 [24] found a moderate positive correlation ( $r=0.58$ ) between WSS measurements and the degree of stenosis. Research has shown that the WSS at the site of stenosis increases, while the WSS at the distal end of stenosis is lower [17]. Lower WSS is usually accompanied by relatively high OSI values [25] and higher blood flow turbulence [26]. A negative correlation between the WSS and blood flow turbulence has been found in peripheral blood vessels [26] and carotid bifurcation [27] based on the V Flow function. Dong et al. 2022 [28] measured the blood flow turbulence of the carotid artery (including the CCA and CB, with ICC above 0.9) in 40 healthy individuals based on the V Flow function. The statistical data showed that the Turbulen. value at CB was significantly higher than that at CCA. This may also confirm why the morbidity of plaque and stenosis at CB is much higher than that at CCA. The main reason may be the complex blood flow with high turbulence caused by the complex structure of CB vessels. Zhao et al. 2022 [29] conducted an animal model study on blood flow turbulence. This study measured the blood flow turbulence of 12 beagle dogs with surgical placement of constrictor rings in the femoral artery. The flow turbulence was measured quantitatively using the V Flow function. The results demonstrated that after the stenotic site, the measured Turbulen. value will increase within a certain distance, and the Turbulen. value at the distal end with higher stenosis rate will also become higher.

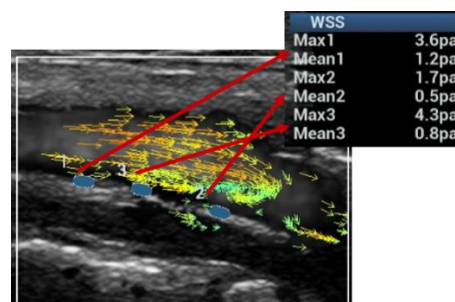


Fig. 12: WSS measurements at the carotid bulb show that the WSS around the vortex is significantly lower than that around the laminar flow

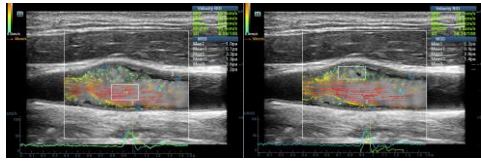


Fig. 13: The measurement of blood flow turbulence at the carotid bulb (CB). Due to the presence of vortices, the Turbulen. value at CB is much higher than that at the laminar flow region (59.2% vs 0.08%); The WSS measurement around the vortex is much lower than that around the laminar flow (0.1Pa vs 1.4Pa).

## Conclusion

The white paper presented a novel visualization for blood flow, in which color arrows are displayed, instead of the color map of a conventional Doppler ultrasound image. The color arrows show both the velocity and direction of the flow, which is also dynamically and intuitively demonstrated when the video is displayed.

Clinical results are showing that the new method gives much more detail with different types of flow in the carotid artery compared to conventional CFM. Various quantitative measurements are provided by V Flow and further extensive clinical research will highlight the real clinical value of using V Flow, and will open new ways for investigation of the pathologies of vessels.

## Acknowledgement

Prof. Alfred CH Yu and Prof. Billy YS Yiu are specially thanked for their distinguished contributions in vector flow imaging techniques. Dr. Alfredo Goddi is appreciated for his valuable clinical support on V Flow application.

## Reference

[1]. C. Kasai, K. Namekawa, A. Koyano and R. Omoto. Real-time two-dimensional blood flow imaging using an autocorrelation technique. *IEEE Transactions on Sonics and Ultrasonics*, 1985; su-32(3):458-464.

[2]. D. J. Phillips, F. M. Greene, Y. Langlois, G. O. Roederer and D. E. Strandness. Flow velocity patterns in the carotid bifurcations of young, presumed normal subjects. *Ultrasound in Medicine & Biology*, 1983; 9:39-49.

[3]. L. Saba. Imaging of the carotid artery. *Atherosclerosis*, 2012; 220:294-309.

[4]. D. P. Giddens, C. K. Zarins, S. Glagov, B. K. Bharadvaj and D. N. Ku. Flow and atherogenesis in the human carotid bifurcation. In: G. Schettler et al, editors. *Fluid dynamics as a localizing factor for atherosclerosis*. Springer-Verlag Press; 1983; pp:38-45.

[5]. H. F. Younis, M. R. Kaazempur-Mofrad, R. C. Chan, A. G. Isasi, D. P. Hinton, A. H. Chau, L. A. Kim and R. D. Kamm. Hemodynamics and wall mechanics in human carotid bifurcation and its consequences for atherogenesis: investigation of inter-individual variation. *Biomechanics and Modeling Mechanobiology*, 2004; 3:17-32.

[6]. T. L. Poepping, R. N. Rankin and D. W. Holdsworth. Flow patterns in carotid bifurcation models using pulsed Doppler ultrasound: effect of concentric vs eccentric stenosis on turbulence and recirculation. *Ultrasound in Medicine & Biology*, 2010; 36(7):1125-1134.

[7]. B. Y. S. Yiu, S. S. M. Lai and A. C. H. Yu, Vector projectile imaging: time-resolved dynamic visualization of complex flow patterns. *Ultrasound in Medicine & Biology*, 2014; 40(9):2295-2309.

[8]. A. C. H. Yu and B. Y. S. Yiu. Apparatus for ultrasound flow vector imaging and methods thereof. WO2015/074511A1.

[9]. B. Y. S. Yiu and A. C. H. Yu. Least-squares multi-angle Doppler estimators for plane wave vector flow imaging. *IEEE Transactions on Ultrasonics, Ferroelectrics, and Frequency Control*, 2016; 63(11):1733-1744.

[10]. Y. Du, R. Fan and Y. Li. Ultrasonic imaging method and system. WO2015/180069A1.

[11]. Y. Du, R. Fan and Y. Li. Ultrasonic blood flow imaging display method and ultrasonic imaging system. WO2016/172890A1.

[12]. Y. Miura, F. Ishida, Y. Umeda, H. Tanemura, H. Suzuki, S. Matsushima, S. Shimosaka and W. Taki. Low wall shear stress is independently associated with the rupture status of middle cerebral artery aneurysms. *Stroke*, 2013; 44:519-521.

- [13]. A. Harloff, S. Berg, A. J. Barker, J. Schollhorn, M. Schumacher, C. Weiller and M. Markl. Wall shear stress distribution at the carotid bifurcation: influence of eversion carotid endarterectomy. *European Radiology*, 2013; 23:3361-3369.
- [14]. A. M. Malek, S. L. Alper, S. Izumo. Hemodynamic shear stress and its role in atherosclerosis. *JAMA*, 1999; 282(21):2035-2042.
- [15]. T. G. Papaioannou, C. Stefanadis. Vascular wall shear stress: basic principles and methods. *Hellenic Journal of Cardiology*, 2005; 46:9-15.
- [16]. J. P. Mynard, B. A. Wasserman, D. A. Steinman. Errors in the estimation of wall shear stress by maximum Doppler velocity. *Atherosclerosis*, 2013; 227:259-266.
- [17]. Y. Du, A. Goddi, C. Bortolotto, Y. Shen, A. Dell’Era, F. Calliada and L. Zhu, Wall shear stress measurements based on ultrasound vector flow imaging. *Journal of Ultrasound in Medicine*, 2020; 39:1649–1664.
- [18]. X. He, D. Ku, Pulsatile flow in the human left coronary artery bifurcation: average conditions. *J Biomech Eng*, 1996, 118:74-82.
- [19]. D. Ku, D. Giddens, C. Zarins, et al. Pulsatile flow and atherosclerosis in the human carotid bifurcation. Positive correlation between plaque location and low oscillating shear stress. *Arteriosclerosis*, 1985, 5:293-302.
- [20]. Y. Du, Y. Shen, B. Y. S. Yiu, A. C. H. Yu and L. Zhu, High frame rate vector flow imaging: Development as a new diagnostic mode on a clinical scanner. *IEEE IUS*, 2018.
- [21]. W. Xu, Y. Du, Y. Liu, X. An, Z. Lu, Y. Liu, S. Li and L. Zhu, Simultaneous measurements of vascular strain and wall shear stress in the carotid artery based on vector flow imaging and vessel wall tracking in duplex mode. *IEEE IUS*, 2022.
- [22]. G. Zahnd, D. Vray, A. Serusclat, D. Alibay, M. Bartold, M. Durand, et al. Longitudinal displacement of the carotid wall and cardiovascular risk factors: Associations with aging, adiposity, blood pressure and periodontal disease independent of cross-sectional distensibility and intima-media thickness. *Ultrasound in Medicine & Biology*, 2012; 38(10):1705–1715.
- [23]. Y. Qiu, D. Yang, Q. Zhang, K. Chen, Y. Dong and W. Wang, V Flow technology in measurement of wall shear stress of common carotid arteries in healthy adults: Feasibility and normal values. *Clinical Hemorheology and Microcirculation*. 2020; 74:453-462.
- [24]. Y. Qiu, Y. Dong, F. Mao, Q. Zhang, D. Yang, K. Chen, S. Shi, D. Zuo, X. Tian, L. Yu and W. Wang, High-frame rate vector flow imaging technique: Initial application in evaluating the hemodynamic changes of carotid stenosis caused by atherosclerosis. *Frontiers in Cardiovascular Medicine*, 2021; 8:617391.
- [25]. J. Ding, Y. Du, R. Zhao, Q. Yang, L. Zhu, Y. Tong, C. Wen and M. Wang, Detection of abnormal wall shear stress and oscillatory shear index via ultrasound vector flow imaging as possible indicators for arteriovenous fistula stenosis in hemodialysis. *Ultrasound in Medicine & Biology*, 2023.
- [26]. D. Song, M. Liu, Y. Dong, S. Hong, M. Chen, Y. Du, S. Li, J. Xu, W. Gao and F. Dong. Investigation on the differences of hemodynamics in normal common carotid, subclavian, and common femoral arteries using the vector flow technique. *Frontiers in Cardiovascular Medicine*, 2022; 9:956023.
- [27]. M. Liu, D. Song, S. Hong, Y. Dong, W. Gao, Y. Du, L. Zhu, J. Xu, F. Dong, Characteristics and correlations of wall shear stress and flow turbulence in the carotid bifurcation evaluated using an ultrasound vector flow imaging. *Journal of Vascular Research*, 2023.
- [28]. Y. Dong, S. Hong, D. Song, M. Liu, W. Gao, Y. Du, J. Xu, F. Dong, Blood flow turbulence quantification of carotid artery with a high-frame rate vector flow imaging. *Journal of Ultrasound in Medicine*, 2022.
- [29]. R. Zhao, H. Zheng, W. Wang, Y. Du, Y. Tong, C. Wen, Quantitative evaluation of post-stenotic blood flow disturbance in canine femoral artery stenosis model: An early experience with vector flow imaging. *Frontiers in Cardiovascular Medicine*, 2022; 9:829825.

**mindray**  
healthcare within reach